# The antiangiogenic agent TNP-470 requires p53 and $p21^{CIP/WAF}$ for endothelial cell growth arrest

**Jing-Ruey J. Yeh*, Royce Mohan*, and Craig M. Crews*†‡**

Departments of *Molecular, Cellular, and Developmental Biology, and †Pharmacology, Yale University, New Haven, CT 06520-8103

Edited by Alfred G. Knudson, Jr., Institute for Cancer Research, Philadelphia, PA, and approved September 15, 2000 (received for review May 19, 1999)

**Targeting the endothelial cell cycle as an antiangiogenic strategy has been difficult given the ubiquitous expression of critical cell cycle regulators. Here, we show that the antiangiogenic drug TNP-470 displays striking cell-type specificity insofar as it induces the expression of $p21^{CIP/WAF}$, a cyclin-dependent kinase inhibitor, in endothelial cells but not in embryonic or adult fibroblasts. Moreover, primary endothelial cells isolated from $p53^{-/-}$ and $p21^{CIP/WAF-/-}$ mice are resistant to the cytostatic activity of TNP-470. We also demonstrate that $p21^{CIP/WAF-/-}$ mice are resistant to the antiangiogenic activity of TNP-470 in the basic fibroblast growth factor corneal micropocket angiogenesis assay. We conclude that TNP-470 induces p53 activation through a unique mechanism in endothelial cells leading to $p21^{CIP/WAF}$ expression and subsequent growth arrest.**

Angiogenesis, or the *de novo* formation of blood vessels from preexisting capillaries, plays an important role in normal physiology (e.g., development, menstruation, and wound healing) and also arises in response to a variety of pathological stimuli (e.g., diabetic retinopathy, rheumatoid arthritis, and tumor growth; ref. 1). Based in large part on the critical role of angiogenesis in tumor growth, much effort has focused on the development of diverse antiangiogenic strategies, many of which target the regulation of endothelial cell homeostasis (2).

Whereas epithelial cells proliferate every 48 h, endothelial cells of the adult vasculature divide less than once per month on average (3, 4). This endothelial quiescence provides an opportunity to target the proliferation of endothelial cells as a means to inhibit pathological angiogenesis. Fumagillin, a fungal metabolite, was discovered based on its potent endothelial cytostatic activity *in vitro* (5). TNP-470, a synthetic derivative of fumagillin, was shown to posses potent antiangiogenic activity and low toxicity in animal studies (5, 6). Based on promising preclinical studies showing that TNP-470 inhibits the growth of solid tumors and prevents their metastasis (7–12), this antiangiogenic compound was one of the earliest to enter antitumor clinical trials (13).

Despite many pharmacological studies, the current knowledge of TNP-470's molecular mode of action is limited. A previous study has shown that TNP-470 exerts biphasic growth inhibition; reversible cytostatic activity toward endothelial cells is observed at low doses (complete growth inhibition at 0.75 nM), but cytotoxic effects are observed at higher concentrations (75 $\mu$M) for all cell types tested (14). The cytostatic inhibition is thought to be responsible for its antiangiogenic effect, because the serum concentration of TNP-470 in rats after systemic administration was much lower than that required for cytotoxic inhibition (14). In addition, incorporation of thymidine, but not uridine and leucine, by human umbilical vein endothelial (HUVE) cells is inhibited by TNP-470 treatment, suggesting specific inhibition of DNA synthesis (14). At the molecular level, TNP-470 does not inhibit early $G_1$ mitogenic events, such as cellular protein tyrosyl phosphorylation or the expression of immediate early genes (15). However, TNP-470 potently inhibits the activation of CDK2 and CDC2 as well as retinoblastoma protein phosphorylation, although not through direct kinase inhibition (15).

CDKs drive cell cycle progression (16) and are in turn regulated at cell cycle checkpoints by CDK inhibitors such as the $p21^{CIP/WAF}$ or $p16^{INK4a}$ family members. These various cell cycle checkpoints are activated by stress and inhibitory signals from the environment. For example, $p21^{CIP/WAF}$ has been shown to be transcriptionally up-regulated by p53 in response to DNA damage, hypoxia, and nucleotide pool perturbation (17) leading to inhibition of retinoblastoma protein phosphorylation and cell cycle arrest at the $G_1$ to S transition (18, 19).

We investigated whether TNP-470 targets one of the CDK inhibitors through a mechanism unique to endothelial cells. Interestingly, we found that endothelial cells treated with nanomolar concentrations of TNP-470 caused the accumulation of the CDK inhibitor $p21^{CIP/WAF}$ protein, correlating with the dose-specific inhibition of endothelial cell growth. We provide further evidence that TNP-470 engages the p53 pathway to exert $p21^{CIP/WAF}$-dependent $G_1$ checkpoint control in endothelial cells. These findings were extended *in vivo* by showing that $p21^{CIP/WAF-/-}$ mice were unresponsive to TNP-470's antiangiogenic activity as measured by the corneal micropocket assay. Finally, we found that growth arrest via this mechanism was not observed in other primary cell types such as fibroblasts, validating the use of TNP-470 as a unique probe to study endothelial cell cycle regulation.

## Materials and Methods

TNP-470 was synthesized as described (20). Antibodies against $p21^{CIP/WAF}$ (C-19), $p27^{KIP}$ (C-19), p53 (FL393), and Mdm2 (SMP14) were purchased from Santa Cruz Biotechnology.

**Cell Culture.** HUVE cells were obtained from J. Pober (Yale Medical School), and bovine aortic endothelial cells (BAE cells) were isolated as described (21). E6-HUVE cells, a primary HUVE cell line with stably integrated human papilloma virus E6 oncogene, was produced as follows. The replication-defective retrovirus containing pLXSN16E6 encoding both the human papilloma virus 16 E6 oncogene and the neomycin resistance gene (22) was produced from a stably transfected packaging cell line kindly provided by S. Lloyd (University of Texas-Southwestern Medical Center, Dallas). After three consecutive 24-h infections in retrovirus-containing medium, stable retroviral integration in HUVE cells was selected in 100 $\mu$g/ml G418 (GIBCO) for 10 days. Murine embryonic fibroblasts (MEFs) were generously provided by T. Williams (Yale University).

This paper was submitted directly (Track II) to the PNAS office.

Abbreviations: HUVE cells, human umbilical vein endothelial cells; CDK, cyclin-dependent kinase; BAE cells, bovine aortic endothelial cells; MPE cells, murine pulmonary endothelial cells; MEF, murine embryonic fibroblasts; bFGF, basic fibroblast growth factor; MetAP, methionine aminopeptidase.

‡To whom reprint requests should be addressed at: Department of Molecular, Cellular, and Developmental Biology, Yale University, 219 Prospect Street, KBT 454, New Haven, CT 06520-8103. E-mail: craig.crews@yale.edu.

The publication costs of this article were defrayed in part by page charge payment. This article must therefore be hereby marked "*advertisement*" in accordance with 18 U.S.C. §1734 solely to indicate this fact.

Murine pulmonary endothelial (MPE) cells were isolated from wild-type mice, $p21^{CIP/WAF-/-}$ mice (23), and $p53^{-/-}$ mice (24) by using a culture medium enrichment method and an immunomagnetic selection protocol modified from L. Richard *et al.* (25). Briefly, anesthetized mice were perfused with PBS and then killed. The lungs were removed, minced, and washed with cold PBS, and tissue was digested in 0.1% collagenase/dispase 1:1 at 37°C for 1 h. Cells were again washed with PBS, and remaining tissue was dissociated by using a loose Dounce homogenizer. The cells were subsequently plated and routinely cultured in RPMI medium 1640 containing 10% (vol/vol) FBS, 5% (vol/vol) platelet-poor horse serum, 2 mM glutamine, 1× Antibiotic-Antimycotic reagent (GIBCO/BRL), 1 mM sodium pyruvate, 2.5 mM Hepes, 25 μg/ml endothelial cell growth supplement (Sigma), and/or 2–10 ng/ml basic fibroblast growth factor (bFGF) (GIBCO/BRL). For the immunomagnetic isolation of MPE cells, anti-E-selectin-coated magnetic beads were prepared by incubating 1.5 μg of rat anti-mouse E-selectin antibody (PharMingen) with 25 μl of Dynabeads M-450 sheep anti-rat IgG (Dynal, Great Neck, NY) overnight at 4°C before use. The beads were washed several times with PBS to remove unbound antibodies and stored at 4°C until needed. Recombinant murine tumor necrosis factor-α (100 ng/ml; GIBCO/BRL) was added to the subconfluent primary cultures to induce the expression of E-selectin, an endothelial cell surface antigen. After 6 h, anti-E-selectin-coated magnetic beads (15 μl/ml) were added, and cultures were incubated with the beads at room temperature with gentle shaking for 2 h. After four washes with PBS, cultures were trypsinized; cells were separated by using a magnet; and after additional washes, E-selectin-positive cells were plated. Isolated endothelial cells were characterized by the uptake of DiI-Ac-LDL (Molecular Probes), positive immunofluorescence staining with rabbit anti-human von Willebrand Factor antibodies (Dako) and Cy3-conjugated anti-rabbit IgG antibodies (Amersham Pharmacia), and immunoblot analyses with anti-Flk1 antibodies (Santa Cruz Biotechnology). Murine adult lung fibroblasts were isolated as follows. Homogenized pulmonary tissues obtained as described above were plated in DMEM with 10% (vol/vol) FBS without selection. HUVE cells, E6-HUVE cells, MPE cells, and MEFs were cultured on tissue culture plates precoated with 0.1% gelatin. BAE cells and MPE cells were cultured at 7% $CO_2$, whereas the other cell lines used were cultured at 5% $CO_2$. BAE cells, murine adult lung fibroblasts, and MEFs were grown in DMEM supplemented with 10% (vol/vol) FBS, 1% penicillin/streptomycin (GIBCO/BRL), and 1 mM sodium pyruvate. HUVE cells and E6-HUVE cells were cultured in M199 supplemented with 20% (vol/vol) FBS, 1% penicillin/streptomycin, and 25 μg/ml endothelial cell growth supplement (Sigma). Unless stated otherwise, BAE cells and MPE cells were serum starved for 72 and 24 h, respectively, to synchronize in $G_0$ and stimulated to proliferate with serum in the presence or absence of TNP-470.

**Western Blot Analysis.** Cells were washed with PBS twice and lysed in RIPA buffer (50 mM Tris, pH 7.5/150 mM NaCl/0.1% Triton X-100/0.5% sodium deoxycholate/0.1 mM EGTA/1 mM EDTA/0.1% SDS/10 μg/ml leupeptin/10 μg/ml pepstatin/1 mM phenylmethylsulfonylfluoride/20 mM NaF/1 mM sodium vanadate). Protein concentrations were determined by BCA assay (Sigma). Equal amounts of proteins were fractionated by SDS/PAGE, transferred to Immun-Blot poly(vinylidene difluoride) membrane (Bio-Rad), and immunoblotted with primary antibodies indicated in each experiment. The bound antibodies were visualized by using peroxidase-conjugated secondary antibodies (Amersham Pharmacia) and an enhanced chemiluminescence detection system (Pierce).

**RNA Isolation and Northern Blots.** Total RNA from the cells was isolated by using the RNeasy kit (Qiagen, Chatsworth, CA). RNA aliquots (5 μg) were electrophoresed on a 1% agarose-formaldehyde (2.2 M) gel and transferred to nylon membrane (Roche Molecular Biochemicals). The membrane was hybridized with $^{32}P$-radiolabeled human $p21^{CIP/WAF}$ cDNA fragment in Rapid-Hyb buffer (Amersham Pharmacia) at 65°C for 2 h. The blot was subsequently washed twice in 2× SSC and 0.1% SDS at room temperature, washed twice in 0.1× SSC and 0.1% SDS at 65°C for 30 min, and exposed to BIOMAX MR film (Kodak).

**Thymidine Uptake Assays.** Cells ($n$ = 1,000) were plated into each well of a 96-well culture plate. After 24 h, the media were replaced, and vehicle (DMSO) or different concentrations of TNP-470 were added for a subsequent 20-h incubation. [Methyl-$^3H$]thymidine (74 kBq; NEN Life Science Products) was then added to each well and incubated for an additional 4 h. Cells were harvested by using a Skatron Cell Harvester, and incorporated radioactivity was quantitated by using liquid scintillation. Each data point is the mean of more than three values.

**Mouse Corneal Micropocket Angiogenesis Assays and Treatment.** $p21^{CIP/WAF-/-}$ mice (Black Swiss/129; a gift from Philip Leder, Harvard Medical School, Boston, MA) and wild-type mice (FVB strain; The Jackson Laboratory) were housed in specific pathogen-free cages. An 80-ng slow-release bFGF pellet was surgically implanted in the corneas of $p21^{CIP/WAF-/-}$ mice ($n$ = 17) or wild-type FVB mice ($n$ = 12) according to the well established procedure of Folkman and coworkers (26). TNP-470 [solubilized in 2% (vol/vol) ethanol-buffered saline] or the vehicle [2% (vol/vol) ethanol-buffered saline] was delivered s.c. (30 mg/kg body weight) every other day to $p21^{CIP/WAF-/-}$ and wild-type mice harboring the bFGF pellets. On day 10, mice were anesthetized, and corneal angiogenesis was quantified by measuring the mean summed length of all new blood vessels as described (27). Student's $t$ test was applied to the data to obtain significance values.

## Results

**TNP-470 Induces $p21^{CIP/WAF}$ Expression in Primary Endothelial Cells.** To investigate the mechanism by which TNP-470 interferes with cell cycle progression, we evaluated the production of $p21^{CIP/WAF}$ and $p27^{KIP}$, two critical inhibitors of CDKs. Because cell cycle arrest induced by TNP-470 has been shown to occur in late $G_1$, a time-course analysis of $p21^{CIP/WAF}$ and $p27^{KIP}$ protein expression was performed. By using BAE cells synchronized by serum starvation, addition of 1 nM TNP-470 resulted in the accumulation of $p21^{CIP/WAF}$ beginning between 4 and 8 h after serum stimulation as evaluated by Western blot analysis. Increased $p21^{CIP/WAF}$ levels reached a plateau at 12 h and continued to be present even 24 h after serum stimulation (Fig. 1*A*). We subsequently determined that TNP-470 did not cause a general effect on cell cycle checkpoint control, because the drug did not alter $p27^{KIP}$ protein levels over the 24-h time period. Meanwhile, no change in $p16^{INK4a}$ expression could be detected on TNP-470 treatment (data not shown). Next, we investigated by mRNA blot analysis whether $p21^{CIP/WAF}$ gene expression was induced by TNP-470. As shown in Fig. 1*B*, incubation of BAE cells with 1 nM TNP-470 for 12 h resulted in accumulation of $p21^{CIP/WAF}$ mRNA by 2-fold over that of vehicle-treated controls. Equal loading of the RNA in each lane was confirmed by hybridization with a glyceraldehyde-3-phosphate dehydrogenase probe. In concert with $p21^{CIP/WAF}$ protein levels, maximum TNP-470-induced $p21^{CIP/WAF}$ mRNA levels were attained after 12 h and remained elevated for at least 24 h (data not shown).

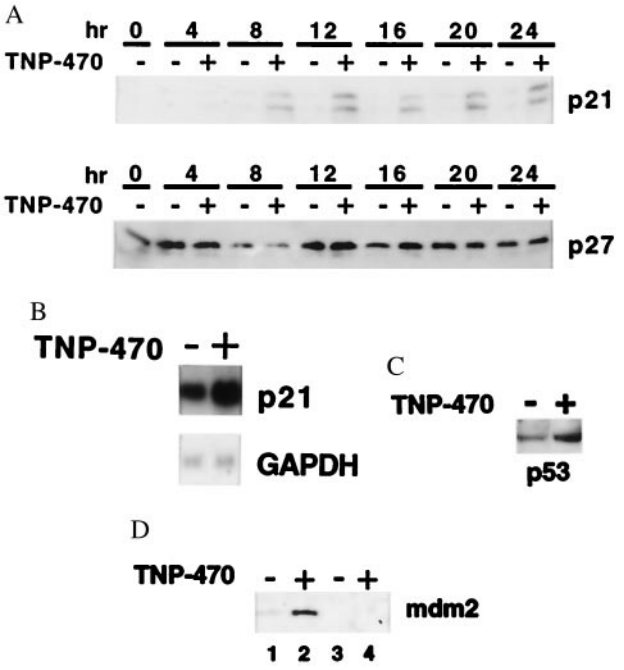


**Fig. 1.** Treatment with TNP-470 results in elevated $p21^{CIP/WAF}$, p53, and Mdm2 levels in endothelial cells. $G_0$ synchronized BAE cells were stimulated with culture medium containing 10% (vol/vol) FBS in presence of vehicle (DMSO) or 1 nM TNP-470 for the indicated amount of time. (*A*) Western blot analysis of 45 $\mu$g of the cell lysates immunoblotted with anti-$p21^{CIP/WAF}$ antisera, stripped and reprobed with anti-$p27^{KIP}$ antibodies. (*B*) Northern blot analysis of $G_0$ synchronized BAE cells serum stimulated in the presence of vehicle or 1 nM TNP-470 for 12 h. Total RNA (5 $\mu$g) was electrophoresed on a 1% agarose-formaldehyde gel and transferred onto nylon membrane. The blot was hybridized with a radiolabeled human $p21^{CIP/WAF}$ cDNA probe, washed, and exposed to x-ray film. Equal loading of RNA was determined by reprobing the blot with glyceraldehyde-3-phosphate dehydrogenase (GAPDH) cDNA. (*C*) Western blot analysis of $G_0$ synchronized MPE cells from wild-type mice stimulated with serum and 10 ng/ml bFGF in the presence of DMSO or 10 nM TNP-470 for 12 h. Lysates (15 $\mu$g) were immunoblotted with p53 antisera. (*D*) Western blot analysis of $G_0$ synchronized MPE cells from wild-type (lanes 1 and 2) and $p53^{-/-}$ (lanes 3 and 4) mice stimulated with serum in presence of DMSO or 10 nM TNP-470 for 12 h. Lysates (30 $\mu$g) were immunoblotted with anti-Mdm2 antisera.

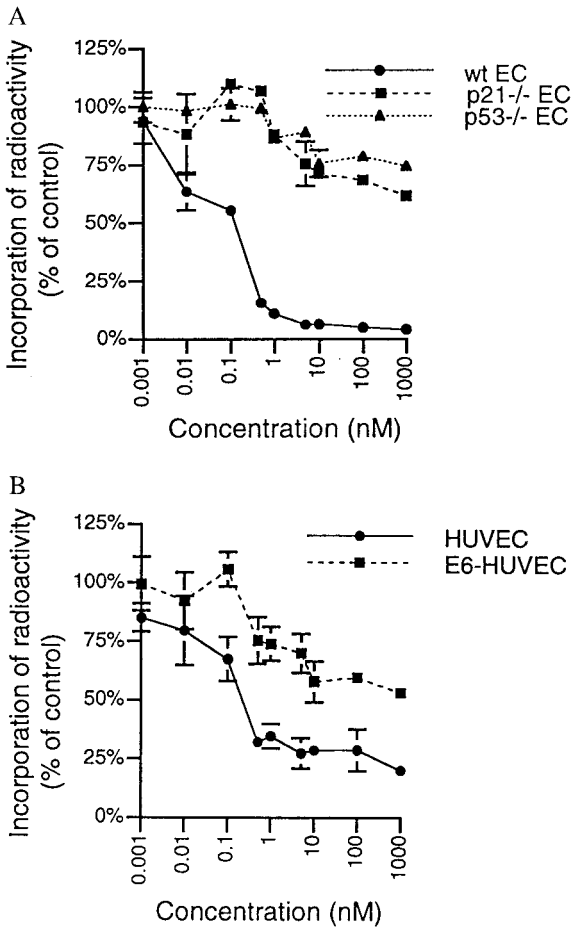


**Fig. 2.** Functional p53 and $p21^{CIP/WAF}$ are essential for TNP-470-induced cell cycle arrest. The effects of TNP-470 on cell proliferation were evaluated by [$^3$H]thymidine incorporation as described in *Materials and Methods*. (*A*) Dose-response curves of MPE cells from wild-type (wt), $p21^{CIP/WAF-/-}$, and $p53^{-/-}$ mice. EC, endothelial cell. (*B*) Dose-response curves of HUVE cells and E6-HUVE cells. Results are presented as the percentage of drug-treated over control (vehicle only) and are shown as the mean and standard deviation of more than three determinants.

**TNP-470 Increases p53 and Mdm2 Protein Levels in Endothelial Cells.** Because $p21^{CIP/WAF}$ levels correlate with TNP-470-mediated cell growth arrest and $p21^{CIP/WAF}$ can be transcriptionally up-regulated by p53, we investigated whether p53 protein levels were induced by TNP-470. Immunoblot analysis of TNP-470-treated MPE cells revealed a 3-fold induction of p53 protein levels in a manner consistent with $p21^{CIP/WAF}$ induction (Fig. 1*C*). Like $p21^{CIP/WAF}$, the Mdm2 gene is transcriptionally downstream from p53 and its mRNA, and protein levels are also known to accumulate with p53 activation under certain conditions (28). Immunoblot analysis of MPE cells revealed that TNP-470 treatment for 12 h also caused Mdm2 protein levels to increase in wild-type but not $p53^{-/-}$ MPE cells (Fig. 1*D*).

**Functional p53 and $p21^{CIP/WAF}$ Are Essential for TNP-470-Induced Endothelial Cell Cycle Arrest.** Because $p21^{CIP/WAF}$ is known to arrest cell cycle progression in late $G_1$ and its levels increase with TNP-470 treatment, we investigated whether TNP-470-mediated cell cycle arrest depended on the presence of $p21^{CIP/WAF}$. To test this mechanism, MPE cells from wild-type and $p21^{CIP/WAF-/-}$ mice were treated with various concentrations of TNP-470 for 20 h and subsequently incubated with [$^3$H]thymidine for 4 h to measure the fraction of cells in S phase. In this experiment, the *y* axis represents the percentage of S phase cells in TNP-470-treated cells versus that in vehicle-treated cells. From the dose-response curve (Fig. 2*A*), the $IC_{50}$ for TNP-470-mediated growth inhibition of MPE cells was calculated to be in the subnanomolar range, an $IC_{50}$ value similar to that of HUVE cells and BAE cells (Fig. 2*B*; see also Fig. 4*A*). In striking contrast, more than 60% of MPE cells from $p21^{CIP/WAF-/-}$ mice continued to proliferate even in the presence of 1 $\mu$M of TNP-470. This finding suggested that a functional $p21^{CIP/WAF}$ was required for the TNP-470 nanomolar concentration-dependent growth inhibition of endothelial cells.

We next investigated whether TNP-470-induced $p21^{CIP/WAF}$-mediated cell cycle arrest was p53-dependent. To abrogate the activities of p53, we used the human papilloma virus 16 E6 gene product, an oncoprotein known to complex with p53 (29) and target it for degradation via the ubiquitin-proteasome pathway (30). By using a retroviral expression vector containing the neomycin resistance gene, we engineered HUVE cells to express E6, and then selected for virus-infected cells using G418. Western blot analyses was performed to confirm that E6-expressing HUVE cells contained no detectable p53 (data not shown). As before, normal HUVE cells and E6-expressing HUVE cells were subjected to [$^3$H]thymidine labeling assays. From the dose-

response curve (Fig. 2*B*), we calculated that the $IC_{50}$ for TNP-470-mediated growth inhibition of HUVE cells was 0.4 nM, whereas the $IC_{50}$ for TNP-470-mediated growth inhibition of E6-expressing HUVE cells was found to be greater than 1 $\mu$M. Although this study suggested that targeting p53 with E6 abrogated TNP-470-mediated growth arrest, it remained a possibility that E6 targeted another essential factor or factors in the TNP-470 signaling pathway. To rule out this possibility, we tested MPE cells from $p53^{-/-}$ mice for TNP-470-induced cell cycle growth arrest in [$^3$H]thymidine labeling assays. As in the studies with E6-expressing HUVE cells, the $IC_{50}$ value of $p53^{-/-}$ MPE cells was greater than 1 $\mu$M. Approximately 70% of the $p53^{-/-}$ MPE cells were resistant to the growth inhibition in the presence of 1 $\mu$M TNP-470, compared with only 5% of the wild-type MPE cells (Fig. 2*A*). Thus, the $p21^{CIP/WAF}$-dependent $G_1$ arrest in endothelial cells caused by TNP-470 was found to require a functional p53. However, p53-independent $p21^{CIP/WAF}$ activation pathways were found to be intact in $p53^{-/-}$ MPE cells as evidenced by increased $p21^{CIP/WAF}$ protein levels in response to the histone deacetylase inhibitor trichostatin A (data not shown). Although p53 activation may induce either cell cycle arrest or apoptosis, and [$^3$H]thymidine labeling assays cannot distinguish cytostatic effects from cytotoxic effects, we determined that endothelial cells treated with 10 nM TNP-470 for 24 h do not undergo apoptosis as measured by the terminal deoxynucleotidyltransferase-mediated UTP end-labeling assay (data not shown).

**$p21^{CIP/WAF}$ Knockout Mice Are Resistant to the Antiangiogenic Activities of TNP-470.** To validate our endothelial cell culture findings in the context of angiogenesis *in vivo*, we used the corneal micropocket neovascularization model to investigate the antiangiogenic activities of TNP-470. Corneas of wild-type and $p21^{CIP/WAF-/-}$ mice were implanted with an 80-ng slow-release bFGF pellet and subsequently treated with either TNP-470 (30 mg/kg body weight) or vehicle on alternate days over a period of 10 days. Corneal blood vessels that approached the bFGF pellet were quantified on day 10 after surgery and revealed by photographic images. As anticipated, in the wild-type strain, TNP-470 treatment ($n = 6$) resulted in a 2.8-fold decrease in the mean summed length of all new corneal blood vessels compared with that of the vehicle-treated group ($n = 6$; $P < 0.03$; Fig. 3*A*). In contrast, there was no significant difference in the angiogenic response of $p21^{CIP/WAF-/-}$ mice between the group treated with TNP-470 ($n = 9$) and vehicle ($n = 8$; $P > 0.5$; Fig. 3*B*). Interestingly, the extent of angiogenesis in untreated $p21^{CIP/WAF-/-}$ mice was considerably reduced relative to that in untreated wild-type mice. However, corneal angiogenesis in $p21^{CIP/WAF-/-}$ mice depended on bFGF, because sucralfate pellets lacking the growth factor failed to exert any angiogenic response (data not shown).

**The Ability to Induce $p21^{CIP/WAF}$ Correlates with Endothelial Cell-Selective Sensitivity to TNP-470.** Sensitivity to TNP-470 differs among cells of different origin. For example, the growth of most tumor cell lines is inhibited by TNP-470 at concentrations three orders of magnitude higher than the concentrations needed to inhibit endothelial cell growth (31). Because immortalization may be a likely event in altering the sensitivities of cells to the cytostatic activity of TNP-470, we explored TNP-470 cell-type-specific sensitivity among primary cells of different origin. Cell proliferation assays were performed by measuring [$^3$H]thymidine incorporation into BAE cells, MEFs, and murine adult lung fibroblasts incubated with various concentrations of TNP-470. As shown in Fig. 4*A*, TNP-470 inhibited the cell cycle progression in these latter two fibroblast cell types with $IC_{50}$ values in the submicromolar range, which was about 1,000-fold higher than the $IC_{50}$ value obtained for endothelial cells. We have also found

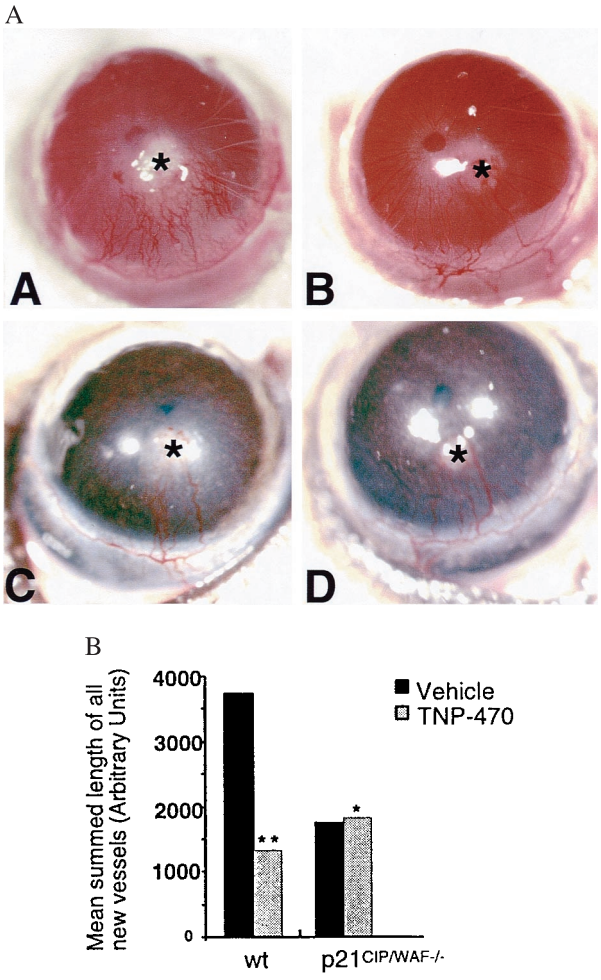


**Fig. 3.** Corneal angiogenesis in $p21^{CIP/WAF-/-}$ mice is not altered by TNP-470 treatment. (*A*) Corneal angiogenesis represented by photographic images of wild-type (*AA* and *AB*) and $p21^{CIP/WAF-/-}$ mice (*AC* and *AD*) 10 days after implantation of slow-release bFGF pellets (asterisk). Mice were treated with TNP-470 (30 mg/kg body weight) (*AB* and *AD*) or vehicle (*AA* and *AC*) on alternate days for the 10-day period. (*B*) Neovascularization was quantified by measuring the summed length of all new blood vessels as described (27). *, $P > 0.5$, vehicle versus TNP-470 ($p21^{CIP/WAF-/-}$); **, $P < 0.03$, vehicle versus TNP-470 (wt, wild type).

that the absence of the p53 or $p21^{CIP/WAF}$ gene in fibroblasts did not make these cells further resistant to TNP-470 in [$^3$H]thymidine uptake assays (Fig. 4*A*). To determine whether the observed nanomolar dose-sensitivity of endothelial cells to TNP-470 depended on the ability to induce $p21^{CIP/WAF}$, we analyzed the induction of this cell cycle regulator in murine primary lung fibroblasts and MPE cells by Western blot analysis. We determined that 10 nM TNP-470 effectively induced $p21^{CIP/WAF}$ protein levels in MPE cells but failed to increase $p21^{CIP/WAF}$ expression in fibroblasts (Fig. 4*B*). We subsequently investigated whether TNP-470-induced $p21^{CIP/WAF}$ expression in endothelial cells was p53-dependent. Western blot analysis of MPE cells from $p53^{-/-}$ mice revealed that TNP-470 treatment failed to induce accumulation of $p21^{CIP/WAF}$ protein, confirming the p53-dependent pathway of $p21^{CIP/WAF}$ induction by TNP-470 (Fig. 4*B*).

## Discussion

In this article, we have shown that the potent angiogenesis inhibitor TNP-470 induces expression of the CDK inhibitor

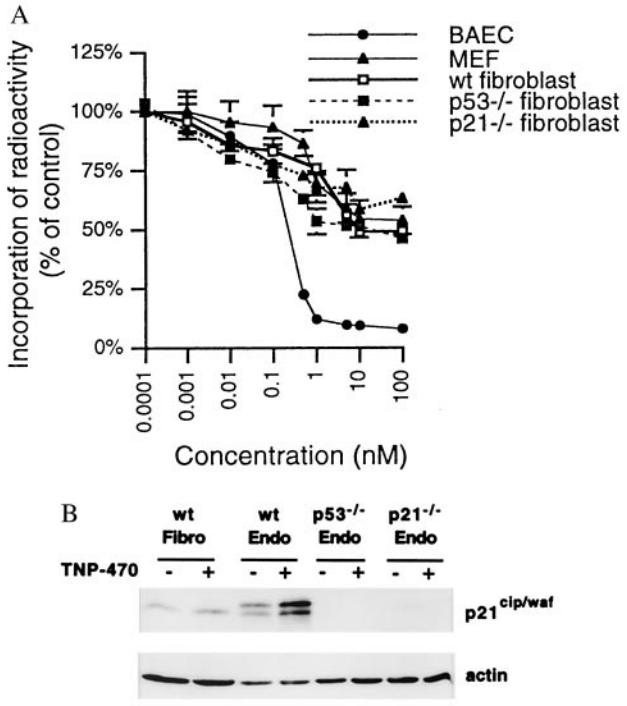


**Fig. 4.** TNP-470-induced $G_1$ arrest and $p21^{CIP/WAF}$ accumulation are not observed in primary fibroblast cells. (*A*) Dose-response curves of BAE cells, MEFs, and murine adult lung fibroblast cells isolated from wild-type (wt), $p53^{-/-}$, and $p21^{CIP/WAF-/-}$ mice treated with TNP-470 were compared by [$^3$H]thymidine incorporation assay. (*B*) Western blot analysis of murine fibroblasts and endothelial (Endo) cells treated with 10 nM TNP-470 for 12 h. Cell lysate (40 $\mu$g) from adult lung fibroblasts and MPE cells from wild-type, $p53^{-/-}$, and $p21^{CIP/WAF-/-}$ mice was loaded in each well. The protein blot was incubated with anti-$p21^{CIP/WAF}$ antisera, and immunoreactive protein was detected by chemiluminescence (*Upper*). The blot was stripped subsequently and reprobed with anti-actin antisera (*Lower*) as a control for protein loading.

$p21^{CIP/WAF}$ and p53 in endothelial cells. Moreover, the function of both $p21^{CIP/WAF}$ and p53 was shown to be essential for the endothelial cell cycle $G_1$ arrest induced by TNP-470. Furthermore, $p21^{CIP/WAF}$ deficiency abrogates the inhibitory activity of TNP-470 on corneal angiogenesis *in vivo*, which is consistent with our cell culture findings. Given these results, $p21^{CIP/WAF}$ induction is most likely the mechanism of the reported inhibition of retinoblastoma protein phosphorylation and the late $G_1$ cytostatic activity of TNP-470 and its parent compound fumagillin (15).

Although $p21^{CIP/WAF}$ and Mdm2 are downstream targets of the transcription factor p53 and are coordinately induced on TNP-470 treatment, the observed 2-fold change in $p21^{CIP/WAF}$ RNA level in 12-h TNP-470-treated endothelial cells does not correspond to the higher change in $p21^{CIP/WAF}$ protein level. This observation suggests that other mechanisms, such as increased translational efficiency or protein stability, may play a role in $p21^{CIP/WAF}$ regulation. However, transcriptional control is involved in $p21^{CIP/WAF}$ induction, because actinomycin D treatment of endothelial cells in the presence of TNP-470 abrogates the TNP-470-mediated up-regulation of $p21^{CIP/WAF}$ expression (data not shown).

Our results establish p53 as a critical component of the TNP-470 signaling pathway in endothelial cells. Evidence for this finding is provided by increased p53 protein levels in response to TNP-470 in a manner consistent with its known transcriptional enhancing activities, the requirement for p53 in $p21^{CIP/WAF}$ and Mdm2 expression, and the requirement for p53 in TNP-470-mediated endothelial cell growth arrest. Although TNP-470 addition results in increased p53 protein levels, it is unlikely that TNP-470 transduces signals to the nucleus through a general genotoxic mechanism, such as DNA damage. This argument is supported by our finding that at concentrations needed to inhibit 90% of endothelial cell growth, TNP-470 inhibited fibroblast proliferation by only 20%. The cell-type selective sensitivity of TNP-470 induced cytostatic activity is intriguing. The requirement for p53 and $p21^{CIP/WAF}$ for TNP-470-induced growth arrest seems to be endothelial cell-specific.

The regulation of p53 can be mediated by several different mechanisms. For example, the Mdm2 gene product has been shown to inhibit p53 through an autoregulatory feedback loop, in which Mdm2 binds the transactivation domain of p53 and inhibits its transactivation activity (32). In addition, Mdm2 also promotes p53 degradation in the cytoplasm by targeting it to the proteasome (33, 34). These negative feedback mechanisms are regulated by phosphorylation of p53 at Ser-15 by both DNA-dependent protein kinase and ataxia-telangiectasia mutated (35–37). Phosphorylation at Ser-15 is believed to disrupt the protein–protein interaction between Mdm2 and p53 and thus neutralize Mdm2-mediated degradation of p53. In TNP-470-treated endothelial cells, both Mdm2 and p53 protein levels increase. Because there is no stoichiometric increase in the phosphorylation status of regulatory serines of p53 with drug treatment, it is unlikely that TNP-470 mediates p53 accumulation via phosphorylation of Ser-6, -9, -15, -20, -37, and -392 (data not shown). However, it is possible that p53 is phosphorylated at other sites in response to TNP-470.

A second major mechanism of regulating p53 accumulation is through the increased expression of the tumor suppressor $p19^{ARF}$, the second gene product of locus INK4a (38). It has been shown that $p19^{ARF}$ stabilizes p53 by forming a tertiary complex with p53 and Mdm2, after which $p19^{ARF}$ targets Mdm2 for degradation (39, 40). In addition, recent studies have also shown that Mdm2 shuttles p53 from the nucleus to the cytoplasm (41) and that $p19^{ARF}$ relocalizes Mdm2 into the nucleolus from the nucleoplasm, thereby preventing Mdm2 binding to p53 (42). Our preliminary data, however, in epitope-tagged Mdm2 and GFP-$p19^{ARF}$ overexpression experiments have failed to show any TNP-470-mediated nucleolar translocation of Mdm2 (data not shown).

The overall extent of bFGF-stimulated angiogenesis in $p21^{CIP/WAF-/-}$ mice was found to be reduced compared with that in wild-type mice. One possibility is that subtle differences in the genetic backgrounds of wild-type and $p21^{CIP/WAF-/-}$ mice could account for the differences in angioproliferative response to bFGF (43). A second possibility takes into account the dual role of $p21^{CIP/WAF}$ in cell cycle regulation. Sherr and coworkers (44) have recently uncovered an additional role for $p21^{CIP/WAF}$ as an "activator" of cell cycle progression, whereby $p21^{CIP/WAF}$ regulates the stability and nuclear localization of D type cyclins and their assembly with CDK4. Thus, it is possible that in $p21^{CIP/WAF-/-}$ mice endothelial cell growth stimulated by the pluripotent mitogen bFGF is partly attenuated, because $p21^{CIP/WAF}$ plays a minor role in cell growth-promoting mechanisms, in addition to its well described major role as a CDK inhibitor.

Although our *in vivo* study indicating the requirement for $p21^{CIP/WAF}$ for inhibition of angiogenesis induced by TNP-470 corroborates our *in vitro* findings on the requirement for $p21^{CIP/WAF}$ for endothelial cell cycle arrest, an important question remains whether TNP-470 induces cell cycle arrest or apoptosis *in vivo*. Pharmacological studies have revealed that the serum concentration of TNP-470 required to exert antiangiogenic activities is in the same range as that needed to promote endothelial cell growth arrest but not cytotoxicity in cell culture (14), in keeping with our findings. Hence, we postulate that the

primary mechanism of TNP-470's antiangiogenic activities is endothelial cell cycle arrest *in vivo*.

The cellular target of TNP-470 is methionine aminopeptidase-2 (MetAP-2), an enzyme responsible for N-terminal processing of methionine residues from polypeptides (45–47). We (45) and others (46) have shown that fumagillin and its derivatives covalently modify and inhibit MetAP-2. The *Saccharomyces cerevisiae* MetAP-2 homolog confers sensitivity to fumagillin/TNP-470-mediated growth arrest *in vivo* when *S. cerevisiae* is deficient in MetAP-1, a related isozyme with a partially redundant function. However, at cytostatic concentrations, fumagillin does not bind to MetAP-1. The molecular basis for the specificity of fumagillin for MetAP-2 over MetAP-1 was elucidated recently through a comparison of the crystal structures of MetAP-2 and MetAP-1, which revealed that the active site of MetAP-1 lacks the appropriate geometry for adduct formation with fumagillin (48).

One possibility for the observed endothelial cell type-selectivity is that these cells lack or express low levels of MetAP-1—analogously to MetAP-1-deficient *S. cerevisiae* that are sensitive to fumagillin/TNP-470—and thus simply require the remaining MetAP-2 activity for growth. Northern blot analysis, however, has shown that there is little difference in the expression levels of MetAP-1 or MetAP-2 between TNP-470-resistant cells (HeLa or HepG2 cells) and TNP-470-sensitive cells (HUVE cells; data not shown). Therefore, the selective sensitivity of endothelial cells is unlikely due to the loss of MetAP-1 expression, or on the other hand, enhanced expression of MetAP-2 in TNP-470-resistant cells. Additionally, we showed that biotinylated fumagillin formed an adduct with MetAP-2 irrespective of the cell type tested, ruling out a possible selective targeting of endothelial cell MetAP-2 by this drug (data not shown). Instead, it is possible that there might be a unique component downstream of MetAP-2 facilitating selective p53 activation in endothelial cells. This model of cell-type-specific p53 regulation is not without precedent. For example, the Wilms' tumor suppressor gene product WT1 is normally expressed in specific precursor cells during a brief period in the developing kidney. Expression of WT1 stabilizes p53, modulates the transcriptional regulation of p53 activities, and inhibits p53-mediated apoptosis (49).

In summary, our study demonstrates the differential TNP-470 responsiveness of primary fibroblasts versus that of endothelial cells. Interestingly, TNP-470 activates p53 and induces $p21^{CIP/WAF}$ expression only in endothelial cells, which accounts for the endothelial-cell-selective growth inhibition by the drug. These findings may prove useful for the development of combinatorial therapies, which target the vascular endothelium.

We thank Jaleel Shujath for assistance with isolation of murine endothelial cells. C.M.C. is a Burroughs–Wellcome Fund New Investigator and a Donaghue Biomedical Foundation Young Investigator. This work was supported by National Institutes of Health Grant CA83049, as well as grants from the Donaghue Biomedical Foundation and Association for the Cure of Cancer of the Prostate.

1. Battegay, E. J. (1995) *J. Mol. Med.* **73,** 333–346.
2. Auerbach, W. & Auerbach, R. (1994) *Pharmacol. Ther.* **63,** 265–311.
3. Engerman, R. L., Pfaffenbach, D. & Davis, M. D. (1967) *Lab. Invest.* **17,** 738–743.
4. Hobson, B. & Denekamp, J. (1984) *Br. J. Cancer* **49,** 405–413.
5. Ingber, D., Fujita, T., Kishimoto, S., Sudo, K., Kanamaru, T., Brem, H. & Folkman, J. (1990) *Nature (London)* **348,** 555–557.
6. Kusaka, M., Sudo, K., Fujita, T., Marui, S., Itoh, F., Ingber, D. & Folkman, J. (1991) *Biochem. Biophys. Res. Commun.* **174,** 1070–1076.
7. O'Reilly, M. S., Brem, H. & Folkman, J. (1995) *J. Pediatr. Surg.* **30,** 325–329.
8. Singh, Y., Shikata, N., Kiyozuka, Y., Nambu, H., Morimoto, J., Kurebayashi, J., Hioki, K. & Tsubura, A. (1997) *Breast Cancer Res. Treat.* **45,** 15–27.
9. Hama, Y., Shimizu, T., Hosaka, S., Sugenoya, A. & Usuda, N. (1997) *Exp. Toxicol. Pathol.* **49,** 239–247.
10. Yazaki, T., Takamiya, Y., Costello, P. C., Mineta, T., Menon, A. G., Rabkin, S. D. & Martuza, R. L. (1995) *J. Neuro-Oncol.* **23,** 23–29.
11. Takamiya, Y., Friedlander, R. M., Brem, H., Malick, A. & Martuza, R. L. (1993) *J. Neurosurg.* **78,** 470–476.
12. Morita, T., Shinohara, N. & Tokue, A. (1994) *Br. J. Urol.* **74,** 416–421.
13. Twardowski, P. & Gradishar, W. J. (1997) *Curr. Opin. Oncol.* **9,** 584–589.
14. Kusaka, M., Sudo, K., Matsutani, E., Kozai, Y., Marui, S., Fujita, T., Ingber, D. & Folkman, J. (1994) *Br. J. Cancer* **69,** 212–216.
15. Abe, J., Zhou, W., Takuwa, N., Taguchi, J., Kurokawa, K., Kumada, M. & Takuwa, Y. (1994) *Cancer Res.* **54,** 3407–3412.
16. Nasmyth, K. (1996) *Science* **274,** 1643–1645.
17. Attardi, L. D. & Jacks, T. (1999) *Cell. Mol. Life Sci.* **55,** 48–63.
18. Zetterberg, A., Larsson, O. & Wiman, K. G. (1995) *Curr. Opin. Cell Biol.* **7,** 835–842.
19. Xiong, Y., Hannon, G. J., Zhang, H., Casso, D., Kobayashi, R. & Beach, D. (1993) *Nature (London)* **366,** 701–704.
20. Marui, S., Itoh, F., Kozai, Y., Sudo, K. & Kishimoto, S. (1992) *Chem. Pharm. Bull.* **40,** 96–101.
21. Garcia-Cardena, G., Fan, R., Stern, D. F., Liu, J. & Sessa, W. C. (1996) *J. Biol. Chem.* **271,** 27237–27240.
22. Wilson, S. E., Weng, J., Blair, S., He, Y. G. & Lloyd, S. (1995) *Invest. Ophthalmol. Visual Sci.* **36,** 32–40.
23. Deng, C., Zhang, P., Harper, J. W., Elledge, S. J. & Leder, P. (1995) *Cell* **82,** 675–684.
24. Jacks, T., Remington, L., Williams, B. O., Schmitt, E. M., Halachmi, S., Bronson, R. T. & Weinberg, R. A. (1994) *Curr. Biol.* **4,** 1–7.
25. Richard, L., Velasco, P. & Detmar, M. (1998) *Exp. Cell. Res.* **240,** 1–6.
26. Kenyon, B. M., Voest, E. E., Chen, C. C., Flynn, E., Folkman, J. & D'Amato, R. J. (1996) *Invest. Ophthalmol. Visual Sci.* **37,** 1625–1632.
27. Mohan, R., Sivak, J., Ashton, P., Russo, L. A., Pham, B. Q., Kasahara, N., Raizman, M. B. & Fini, M. E. (2000) *J. Biol. Chem.* **275,** 10405–10412.
28. Freedman, D. A., Wu, L. & Levine, A. J. (1999) *Cell. Mol. Life Sci.* **55,** 96–107.
29. Maki, C. G., Huibregtse, J. M. & Howley, P. M. (1996) *Cancer Res.* **56,** 2649–2654.
30. Scheffner, M., Huibregtse, J. M., Vierstra, R. D. & Howley, P. M. (1993) *Cell* **75,** 495–505.
31. Castronovo, V. & Belotti, D. (1996) *Eur. J. Cancer* **32,** 2520–2527.
32. Chen, J., Lin, J. & Levine, A. J. (1995) *Mol. Med.* **1,** 142–152.
33. Kubbutat, M. H., Jones, S. N. & Vousden, K. H. (1997) *Nature (London)* **387,** 299–303.
34. Haupt, Y., Maya, R., Kazaz, A. & Oren, M. (1997) *Nature (London)* **387,** 296–299.
35. Shieh, S. Y., Ikeda, M., Taya, Y. & Prives, C. (1997) *Cell* **91,** 325–334.
36. Canman, C. E., Lim, D. S., Cimprich, K. A., Taya, Y., Tamai, K., Sakaguchi, K., Appella, E., Kastan, M. B. & Siliciano, J. D. (1998) *Science* **281,** 1677–1679.
37. Banin, S., Moyal, L., Shieh, S., Taya, Y., Anderson, C. W., Chessa, L., Smorodinsky, N. I., Prives, C., Reiss, Y., Shiloh, Y., *et al.* (1998) *Science* **281,** 1674–1677.
38. Kamijo, T., Zindy, F., Roussel, M. F., Quelle, D. E., Downing, J. R., Ashmun, R. A., Grosveld, G. & Sherr, C. J. (1997) *Cell* **91,** 649–659.
39. Zhang, Y., Xiong, Y. & Yarbrough, W. G. (1998) *Cell* **92,** 725–734.
40. Pomerantz, J., Schreiber-Agus, N., Liegeois, N. J., Silverman, A., Alland, L., Chin, L., Potes, J., Chen, K., Orlow, I., Lee, H. W., *et al.* (1998) *Cell* **92,** 713–723.
41. Tao, W. & Levine, A. J. (1999) *Proc. Natl. Acad. Sci. USA* **96,** 3077–3080.
42. Weber, J. D., Taylor, L. J., Roussel, M. F., Sherr, C. J. & Bar-Sagi, D. (1999) *Nat. Cell Biol.* **1,** 20–26.
43. Rohan, R. M., Fernandez, A., Udagawa, T., Yuan, J. & D'Amato, R. J. (2000) *FASEB J.* **14,** 871–876.
44. Cheng, M., Olivier, P., Diehl, J. A., Fero, M., Roussel, M. F., Roberts, J. M. & Sherr, C. J. (1999) *EMBO J.* **18,** 1571–1583.
45. Sin, N., Meng, L., Wang, M. Q., Wen, J. J., Bornmann, W. G. & Crews, C. M. (1997) *Proc. Natl. Acad. Sci. USA* **94,** 6099–6103.
46. Griffith, E. C., Zhuang, S., Turk, B. E., Chen, S., Chang, Y.-H., Wu, Z., Biemann, K. & Liu, J. O. (1997) *Chem. Biol.* **4,** 461–471.
47. Turk, B. E., Griffith, E. C., Wolf, S., Biemann, K., Chang, Y. H. & Liu, J. O. (1999) *Chem. Biol.* **6,** 823–833.
48. Liu, S., Widom, J., Kemp, C. W., Crews, C. M. & Clardy, J. (1998) *Science* **282,** 1324–1327.
49. Maheswaran, S., Englert, C., Bennett, P., Heinrich, G. & Haber, D. A. (1995) *Genes Dev.* **9,** 2143–2156.